Kufa Journal of Engineering
Vol. 16, No. 4, October 2025, P.P. 268-287
Article history: Received 7 December 2024, last revised 9 January 2025, accepted 26 January 2025

FLEXURAL BEHAVIOR OF STEEL AND GFRP-REINFORCED LIGHTWEIGHT CONCRETE HOLLOW ONE-WAY SLABS UNDER HIGH TEMPERATURES

Hussein M. Kareem [1,2] and Assim M. Lateef [3]

[1] Graduate PhD. student, Civil Engineering Department, Tikrit University, Iraq.

[2] Asst. Lect., Architecture and building Department, Technical Engineering College/Kirkuk, Northern Technical University, Iraq,Email:husseinmudher@ntu.edu.iq

[3] Prof., Civil Engineering Department, Tikrit University, Iraq, Email:assaim77@tu.edu.iq

https://doi.org/10.30572/2018/KJE/160416

ABSTRACT

The purpose of this research is to evaluate the impact of different reinforcements, hollow shapes, and fire on ten lightweight concrete slabs that are reinforced with glass fiber reinforced polymer (GFRP) in order to decrease their weight. All slabs were uniformly sized at 2400 mm x 1000 mm x 150 mm. They were subjected to continuous static load tests and heated from below using a fire chamber to evaluate their fire resistance performance. The study analyzed three reinforcement types (steel, hybrid, and GFRP) and two hollow shapes (circular and square). The findings showed that increasing the GFRP reinforcement ratio and the presence of hollows led to diminished fire resistance and flexural strength compared to solid reinforced concrete slabs. Specifically, the quantity of GFRP reinforcement increased the slabs' deflection, up to a maximum increase of 1.5 times that of the steel-reinforced slab. The slabs' ultimate capacity dropped by around 35% in terms of load capacity. The decrease in stiffness was much more noticeable. Experimental fire exposure results indicated that slabs reinforced with GFRP bars exhibited significant degradation after just over fifty minutes, contrasting with solid reinforced concrete slabs, which withstood the two-hour test. The core focus of this research is to characterize the structural response of GFRP-reinforced lightweight hollow slabs subjected to concurrent fire and stress. The computational models created herein also provide a basis for future analysis, enabling the evaluation of different fire scenarios on specific structural elements or the holistic simulation of a full structural system with realistic boundary conditions.

KEYWORDS

Exposed fire; GFRP bar; Hollow slabs; Lightweight concrete; One-way slab.

1. INTRODUCTION

The building industry has been impacted globally by the rising expense of traditional aggregates and the increasing environmental concerns. The ability of light weight concrete (LWC) to lower concrete weight and address the issue of excessive self-weight in high building is its most well-known feature (Momtazi et al., 2015). Reducing the weight of the structure is likely to lead to construction with fewer parts, which would make the construction process more accessible and cost-effective(Jasim and Jabal, 2010). Utilizing lightweight concrete in the construction of high-rise/multi-story buildings can lead to a decrease in construction expenses. Moreover, the utilization of lightweight concrete can reduce the cross-section of structural components (Sajedi and Shafigh, 2012). Studies conducted by (Jomaa'h et al., 2018; Jomaa'h et al., 2019) illustrate how several one-way reinforced concrete slab designs may be made using lightweight aggregates. Lightweight concrete was created by substituting certain replacement ratios of thermostone and claystone (bonza) for coarse particles. The results showed a reduction in dead weight due to the lightweight aggregates, with optimal performance achieved when 75% of the normal aggregate was replaced with thermostone, resulting in low density with acceptable compressive strength.

Many studies have incorporated various void geometries, including ball, rectangular and cubic shapes, alongside differing strengths and loading conditions (Nimnim and Zain Alabdeen, 2021; Badawi et al., 2023). Similar to one-way ribbed slabs, hollow slabs made up of a number of ribs gain resistance. This is so because the bending resistance in relation to the positive moment is unaffected by the removal of the concrete between the ribs. This is because, even though it is there, the analysis ignores the concrete under the neutral axis since it is under strain. (Setareh and Darvas, 2017; Salih et al., 2023).

Fibers combine textiles with a polymeric network to form composite materials; they are frequently made of glass, carbon, aramid, or basalt. These fibers' unique characteristics make them perfect for strengthening and constructing (Ftnan and Makki, 2022; Ibrahim and Lateef, 2024). When coupled with concrete, they have extraordinary properties that produce powerful compounds, increasing the durability and strength of the concrete1212 (Hibtallah and K. Madlum, 2022). And the types of fiber-reinforced polymer: Glass fiber-reinforced polymers (GFRP) have recently gained significant attention in civil engineering due to their many advantages over traditional materials such as steel. These benefits include high strength, low weight, and resistance to electrochemical corrosion (Murthy et al., 2020). Additionally, the lower costs associated with GFRP reinforcement in construction have made it a more competitive option in civil engineering projects. Nowadays, GFRP reinforcing bars are widely used in industrial, medical, and research facilities as well as retaining walls, bridge decks, and floor slabs (Rosa et al., 2023).

The mechanical and thermal characteristics of Fiber Reinforced Polymer (FRP) are greatly affected by temperature, with even a slight increase (between 100 and 200 °C) leading to significant declines in mechanical properties (Bisby, 2003). The fire resistance of FRP-reinforced components is influenced by several elements, such as the type of reinforcement, the type of aggregates, the design of hollows, and the thickness of the concrete cover. Different FRP materials show varying levels of mechanical and bonding degradation under high temperatures, making the choice of reinforcement crucial. Additionally, the type of aggregate, which makes up a substantial part of concrete, significantly impacts heat transfer to the reinforcement, thereby affecting the temperature transfer at the bar attachment points during a fire (ACI 440. 1R-15, 2015).

Studies have linked fire resistance to GFRP-reinforced normal-weight concrete members. Such studies have examined GFRP-specific challenges in establishing design codes for FRP-reinforced concrete members. The effects of high temperatures on reinforced concrete beams reinforced with GFRP bars were assessed in a research by (Abdullah and Kassim, 2024). The experimental work on GFRP RC beams demonstrated significant deflection at elevated temperatures. The temperature of GFRP bars increases gradually under high heat. GFRP bar achieved its maximum temperature of 355 °C when the beams were heated to 800 °C for 60 minutes. GFRP RC beams exhibited flexural fractures after 90 minutes of exposure to temperatures exceeding 800 °C. (Tanano et al., 1995) FRP-reinforced concrete beams' maintained strength was evaluated at high temperatures. As the heating temperature rises, the epoxy matrix bonding in FRP concrete beams diminishes. Heating up to 250 °C has no effect on FRP inorganic matrix beams. High temperatures reduced the residual tensile strength in all FRP reinforcement. The fire resistance of GFRP-reinforced concrete components has not been well studied, and issues are exacerbated by the rapid loss of GFRP bars' mechanical and bonding properties at high temperatures. As a result, inadequate suggestions on fire design were supplied (Rosa et al., 2023).

Structures are exposed to different fire intensities during fire testing, which may be done in actual buildings or within a furnace. The evaluation of the fire resistance of structural components is most often conducted by furnace testing.

The application of GFRP reinforcement in one-way structural slabs under combined fire and load conditions remains an under-explored area. The present work therefore focuses on characterizing the structural performance of GFRP-reinforced lightweight hollow concrete slabs when subjected to simultaneous stress and high temperatures.

2. EXPERIMENTAL PROGRAMS

2.1. Specimen material

Lightweight concrete is used in this investigation. Concrete mixtures are designed using the American Method (Standard, 1996). The theoretically necessary amounts were first determined: 450 kg/m3 of cement, 711 kg/m3 of sand, a mixing ratio of 1: 1.58: 2.14, and w/c (0.435) equivalent to 195 kg were employed. In order to achieve lightweight concrete, the light-weight coarse aggregate claystone (Bonza) was substituted for the standard coarse aggregates (963 kg/m3), accounting for 66% of the volume of normal coarse aggregate. Because coarse and light-weight coarse aggregates have different specific weights, volumetric replacement ratios were used rather than weight replacement. A two-size deformed steel and GFRP reinforcement bars was employed to strengthen the slabs. Steel bars with a 10 mm diameter and GFRP bars with an 8 mm diameter were used. Table 1 displays the hardened characteristics of lightweight concrete.

Table 1.Hardened characteristics of lightweight concrete.

Mix.	Compressive Strength [Mpa]	Splitting tensile strength [Mpa]	Flexural strength [Mpa]	Density [Kg/m^3]
LWC	17.9	2.12	4.32	1815

2.2. Description of slabs

Ten slab specimens were cast; each specimen measures the same (2400 mm x 1000 mm x 120 mm), and the area of reinforcement (GFRP) uses (8 mm @ 250 mm), while the region of standard reinforcement uses (10 mm @ 250 mm) in each direction. Along its length, the slab included hollow interiors of varying shapes, both square and circular. A concrete cover of 25 mm was selected. An indirect control fire was applied to nine slab samples, and they burned continuously for two hours. One of these samples, known as the reference sample, was not exposed by the fire. The components of the reinforced concrete slab are shown in detail in Fig. 1, and Table 2 details the quantities and configurations of the tested specimens.

Table 2. gives information on the amounts and configurations of the tested specimens.

No.	Groups	Symbols	Type Reinforcement	Shapes hollow	Temperature
1	--------	LSS	Steel (10 mm @ 250 mm)	Sold	At the ambient
2	Group 1	LSS	Steel (10 mm @ 250 mm)	Sold	Temperature according to ASTM-E119
3		LSC	Steel (10 mm @ 250 mm)	Circular	
4		LSQ	Steel (10 mm @ 250 mm)	Square	
5	Group 2	LHS	Hybrid /Steel (10 mm @ 250 mm) GFRP (8 mm @ 250 mm)	Sold	Temperature according to ASTM-E119
6		LHC	Hybrid /Steel (10 mm @ 250 mm) GFRP (8 mm @ 250 mm)	Circular	
7		*LHQ	Hybrid /Steel (10 mm @ 250 mm) GFRP (8 mm @ 250 mm)	Square	
8	Group 3	LGS	GFRP (8 mm @ 250 mm)	Sold	Temperature according to ASTM-E119
9		LGC	GFRP (8 mm @ 250 mm)	Circular	
10		LGQ	GFRP (8 mm @ 250 mm)	Square	

*LHQ: L: Lightweight concrete, S: Steel Reinforcement, Q: SQuare hollow

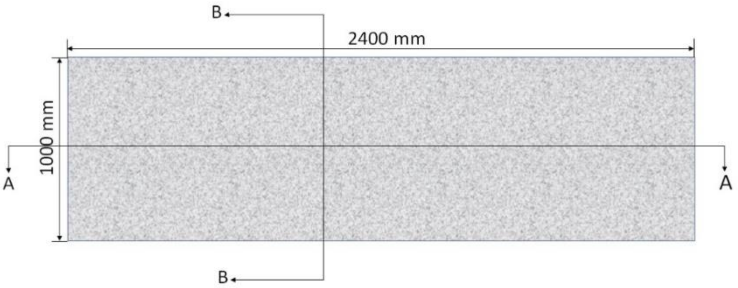

a-Top view of a reinforced concrete slab.

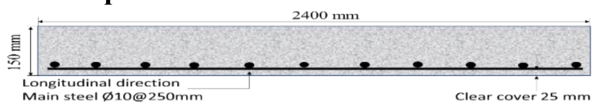

b- Section A-A: Side view of a slab of reinforced concrete

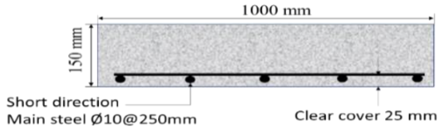

c- Section B-B : shows the side view of a reinforced concrete slab.

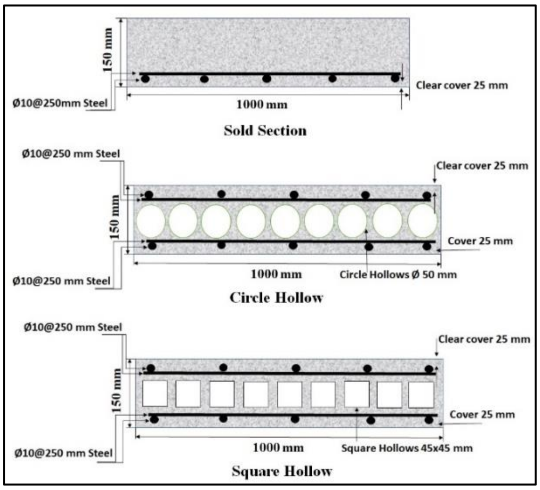

1-Group (1) (3 Sample) Steel Reinforcement.

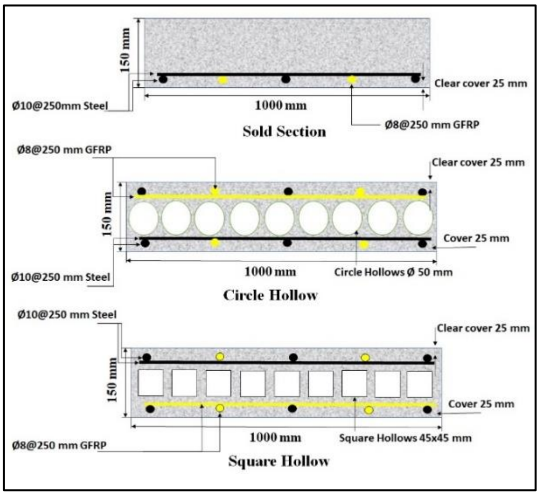

2- Group (2) (3 Sample) Hybrid Reinforcement

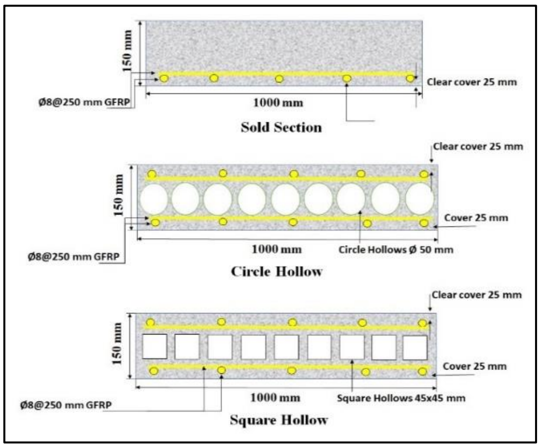

3- Group (3) (3 Sample) GFRP Reinforcement

d- Cross sections of the distribution for reinforcement and hollows.

Fig. 1. Displays the elements of the reinforced concrete slab in great detail

2.3. Test Setup

2.3.1. Fire Loading

Researchers in the field predominantly utilize the fire testing protocol established by ASTM E 119, as it is the most commonly endorsed and applied standard for evaluating the performance of building structures and materials under fire conditions (Chaturvedi et al., 2022). It is the procedure that is most commonly used and approved. This study uses gas burners to heat the furnace. The slab specimens undergo controlled bottom fire exposure for a duration of 2 hours. The temperature in the furnace rises in accordance with the time-temperature curve established in the (ASTM E 119) standard, the test involved subjecting the specimen to a standardized ASTM E 119 fire curve for a defined period, as shown in Fig. 2. During the experiment, three thermocouples provided immediate temperature feedback from the combustion chamber, enabling precise regulation of the thermal environment to maintain compliance with the standard. The fire chamber's configuration is detailed in Fig. 3-a.

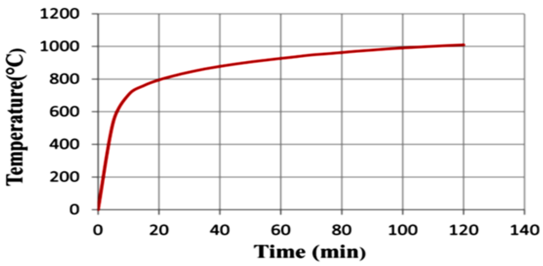

Fig. 2.Standard time-temperature curve (Chaturvedi et al., 2022).

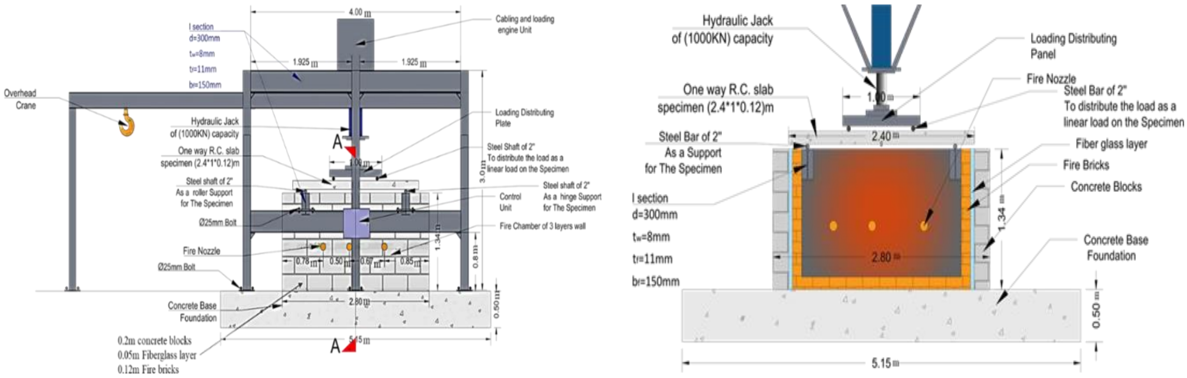

a- Fire chamber is shown in detail in the longitudinal section (Klak and Jomaa'h, 2024).

b- Loading the sample over the combustion chamber.

Fig.3. Shows the detail section of the fire chamber.

2.3.2. Flexural Load Test

2.3.2.1. Flexural Strength Test for Reinforced LWC Slabs at the ambient temperature

The reference slab under test is placed horizontally along the length of the furnace, as illustrated in Fig. 3-b. A hydraulic jack with a maximum load capacity of 1000 KN supports the slab. The jack moves the load onto the slab and spreads it out over two lines. The LVDT is located in the slab's center and records both mid-span deflection measurements and applied force. The load is applied till failure occurs, after which the ultimate load is recorded by taking 50% of it to be used in the thermal examination, according to (Al-Attar et al., 2020).

2.3.2.2. Flexural Strength Test for Reinforced LWC Slabs Under Fire Exposure

Through their long sides parallel to the furnace's borders, the tested slabs are positioned horizontally across the furnace's aperture. Then, to provide a direct line load, two shafts were loaded directly above the slab specimen. The specimen was fastened to the fundamental supports and flexural testing apparatus. Prior to burning, a hydraulic jack gradually loads the slab, measuring deflection in the center of the span until it achieves 50% of the ultimate load. The slabs from each group were then heated to a high temperature for 120 minutes, or until failure, in accordance with ASTM E 119. Fig. 4 shows the test equipment.

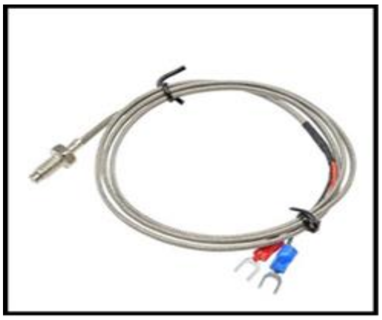

Thermocouple type K.,

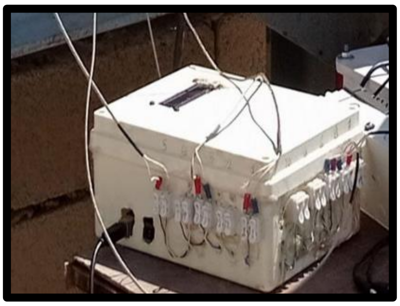

(b) Temperature indicator

(c) Data Logger

(d) LVDT

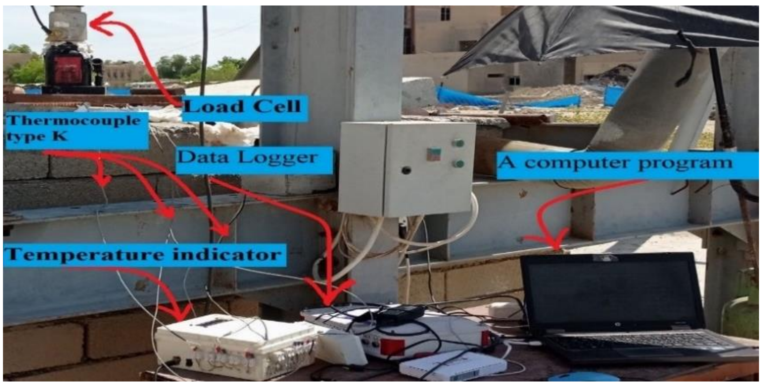

(e) Total devices used

Fig. 4. Devices and sensors for examination.

3. RESULTS AND DISCUSSION

3.1. Temperature profiles

Fig. 5 illustrates the positions of the thermocouple in four primary places in each sample where the temperature was recorded during the firing stage.

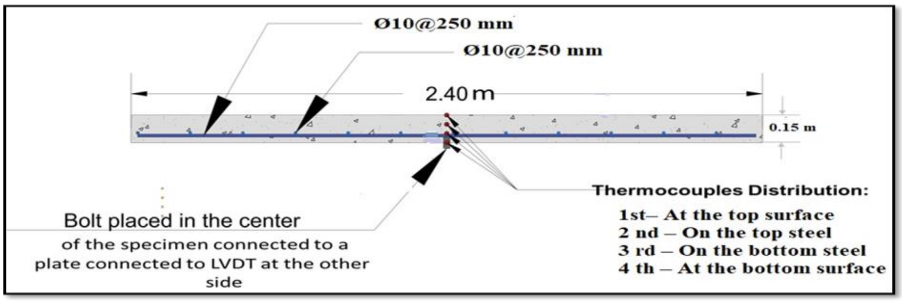

Fig.5. Locations of the thermocouple sensors are in the middle region of the slab specimen.

The temperature profiles recorded during the fire resistance tests are shown in Fig. 6a for steel-reinforced slabs, Fig. 6b for hybrid-reinforced slabs, and Fig. 6c for GFRP-reinforced slabs. The temperatures were recorded (at midspan) at four positions in slabs. The thermocouple near the slabs' bottom surface closely matched the conventional fire curve (ASTM E 119, 2018). Temperatures consistently rose over time across all thermocouples, although at varying speeds. As anticipated, the temperature dropped from the bottom to the top of the slabs; during the same duration (60 minutes), the steel-reinforced slabs' bottom and top surfaces had a temperature differential of 788 °C, the hyprid-reinforced slabs' was 735 °C, and the GFRP-reinforced slabs' was 709 °C. In all slabs, when the concrete temperature neared 100 °C, the heating rates significantly decreased (subsequently rising again after a few minutes) owing to moisture evaporation. Furthermore, the observations from thermocouples positioned symmetrically along the longitudinal axis exhibited similar readings in the fire chamber. The fact that the concrete is not uniform throughout, the temperature sensors are not all in the same location, or cracks developed or opened up during the tests can all account for the minor differences that were visible, particularly in the middle section.

3.2. Fire and static load effects on reinforced LWC slabs.

This study examines the flexible behavior of one way hollow reinforced lightweight concrete slabs under simultaneous static loads and fire conditions. Every slab of reinforced concrete with the three groups has the same hollows (square and circular), the same reinforcement ratio, and the same dimensions. Consequently, the load-deflection curve in the center of the slab will be used to present the test results, and the general behavior of one-way reinforced hollow lightweight concrete slabs will be explained., along with the calculation of the first cracking load, maximum load, ductility, and stiffness.

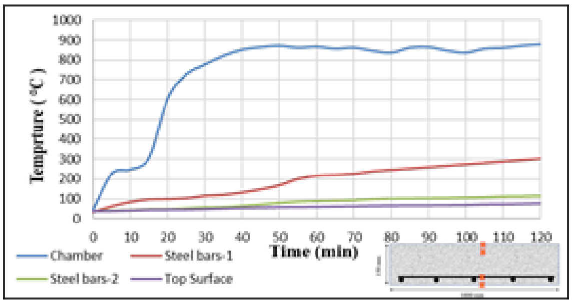

a-1 : Temperature distribution for slab LSS.

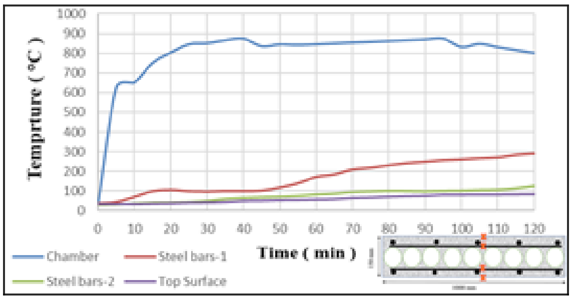

a-2 : Temperature distribution for slab LSC

Group -1- Temperature distribution for Steel reinforced slabs.

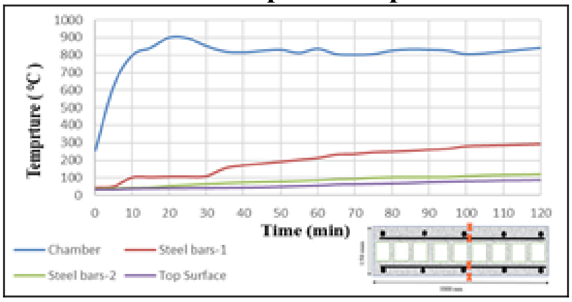

a-*3* : Temperature distribution for slab LSQ .

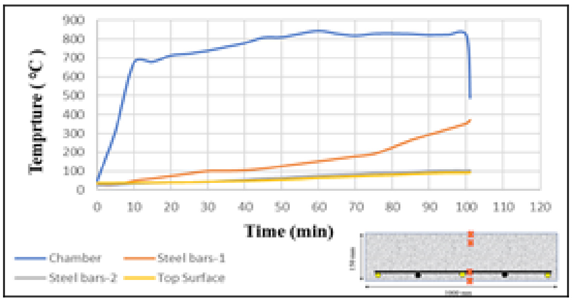

b-1 : Temperature distribution for slab NHS.

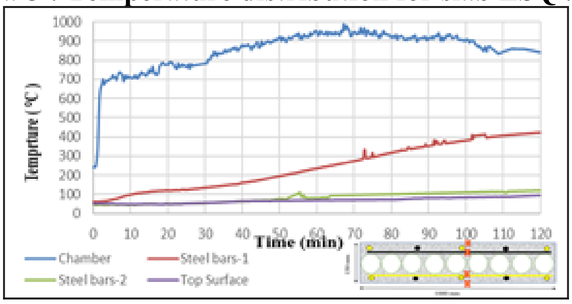

b-2: Temperature distribution for slab LHC.

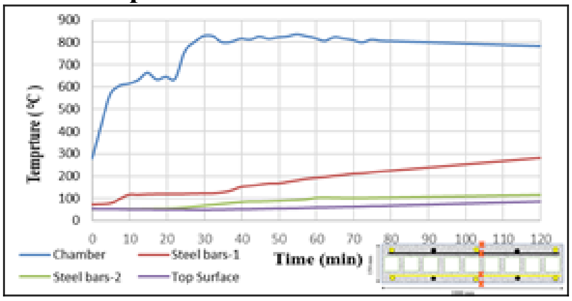

b-3: Temperature distribution for slab LHQ.

Group -2- Temperature distribution for hybrid reinforced slabs

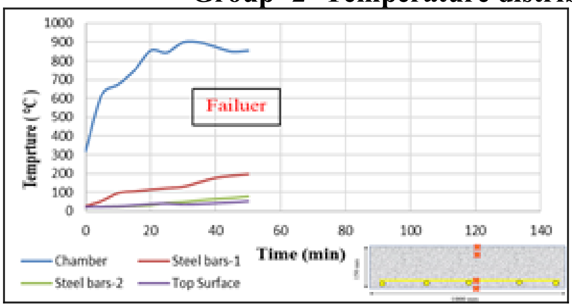

c-1 : Temperature distribution for slab LGS.

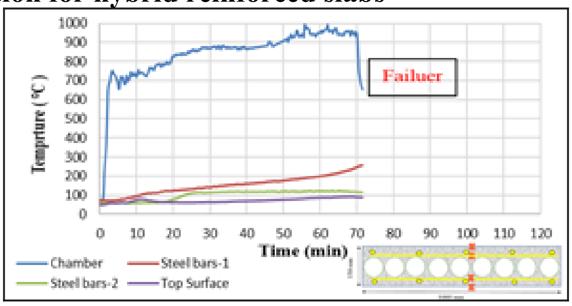

c-2 : Temperature distribution for slab LGC

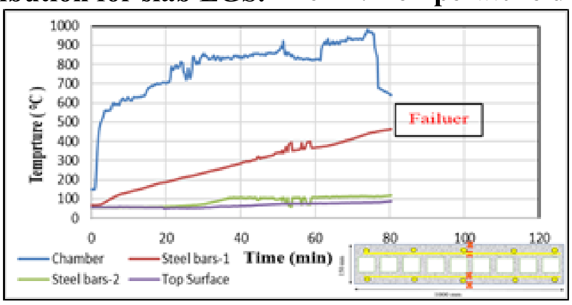

c-3: Temperature distribution for slab LGQ.

c- Group -3- Temperature distribution for GFRP reinforced slabs.

Fig. 6. Temperature distribution for slabs.

3.2.1. First Crack and Deflection.

The first cracking load and corresponding deflection for the one-way hollow lightweight concrete slabs were identified visually upon the appearance of the initial crack, with the load being recorded at that moment. These values are displayed in Table 3.

A comparison of the flexural test results Fig. 7 for the hollow slabs (LSC, LSQ, LHC, LHQ, LGC, LGQ) with the solid reference slabs (LSS, LHS, LGS) revealed a progressive reduction in initial cracking resistance with the introduction of hollow sections. The cracking load values for the hollow slabs increased by between 2.24% and 41.62% compared to the reference slabs. Conversely, their deflection values decreased by between 2.45% and 36.9%. The first flexural crack occurred at various applied stress levels, ranging from 9.8 kN to 75.44 kN.

The observed reduction in structural performance is a consequence of the smaller effective concrete area in tension, which is loaded from the outset of the experiment. Furthermore, results demonstrated an inverse relationship between the GFRP reinforcement percentage and the load at which the first crack formed under static and fire loads. A key distinction was noted in the timing of the first crack: it emerged at roughly half the failure load in pre-fire tests for GFRP slabs, while for their steel-reinforced counterparts, cracking initiated only after fire exposure began.

Table 3. First crack and deflection in hollow reinforced concrete slabs.

Group	Symbols	Type of Reinf.	Shape of hollow	P_{cr} (KN)	δ_{cr} (mm)	(Variation percentage P_{cr})%	(Variation percentage δ_{cr}) %	Fire time (min)
–	LSS	Steel	Sold	40.3	8.9	____	____	____
Group 1	LSS	Steel	Sold	58.15	10.35	Reference	Reference	9
	LSC	Steel	Circular	75.44	6.78	29.73	-34.49	16
	LSQ	Steel	Square	61.14	10.02	5.14	-3.18	10
Group 2	LHS	Hybrid	Sold	50.37	13.57	Reference	Reference	5
	LHC	Hybrid	Circular	71.33	8.56	41.63	-36.91	10
	LHQ	Hybrid	Square	69.44	10.5	37.98	-22.63	8
Group 3	LGS	GFRP	Sold	9.81	10.17	Reference	Reference	Before fire
	LGC	GFRP	Circular	10.36	9.64	5.62	-5.22	Before fire
	LGQ	GFRP	Square	10.03	9.92	2.25	-2.44	Before fire

3.2.2. Ultimate Load-Deflection Relationship for Hollow Reinforced LWC Slabs.

The experimental procedure was conducted in two distinct stages. Initially, a two-point loading system was employed, applying force up to a service load of 36 kN. The mid-span deflection was meticulously documented at each load increment. Subsequently, the slabs were subjected to a fire exposure phase, heated by gas burners that followed the ASTM E 119 standard time-temperature curve for a duration of 120 minutes.

Data on deflection as a function of fire exposure, detailed in Table 4 and Fig.8, revealed that a higher GFRP reinforcement ratio correlated with reduced fire resistance and earlier failure times. The slabs reinforced with GFRP (LGS, LGC, LGQ) failed after 50, 80, and 70 minutes, respectively. In contrast, the reference slabs reinforced with steel and hybrid reinforcement withstood the entire 120-minute fire test without failure.

Furthermore, the load-deflection curves for the hollow-core slabs demonstrated a less steep slope compared to the solid reference slabs. This is a direct consequence of the hollow sections reducing both the maximum load capacity and the initial cracking load. To mitigate this structural weakening, a second layer of reinforcement was introduced in the tension zone. This compensatory measure is anticipated to improve the ultimate load capacity and reduce deflections relative to the standard hollow-core slabs.

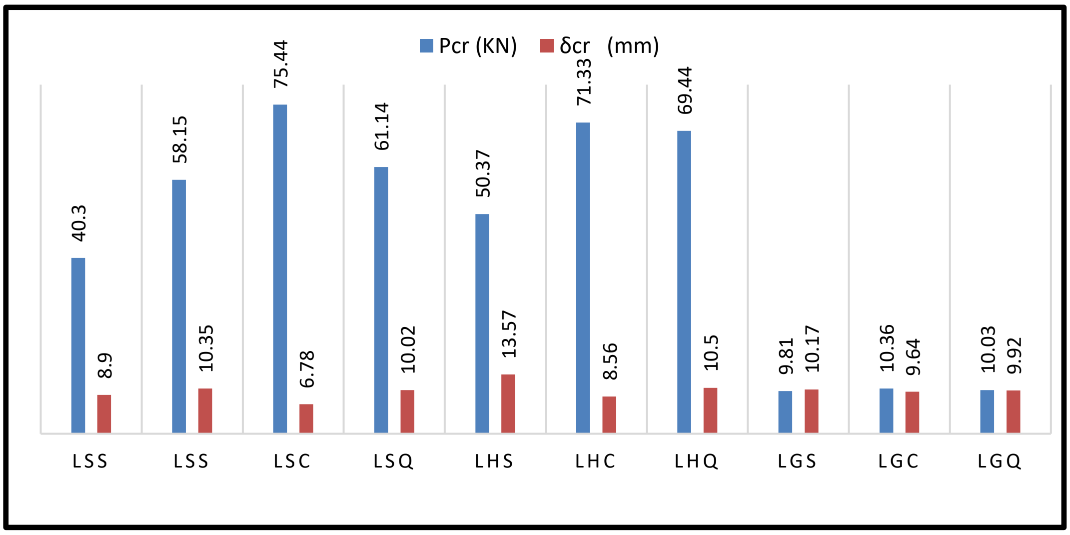

Fig. 7. First cracking and deflection measurements on slabs.

Table 4: Ultimate load and deflection in hollow reinforced LWC slabs.

Group	Symbols	Type of Reinf.	hape of ollow	P_{cr} (KN)	δ_{cr} (mm)	(Variation percentage P_{cr})%	(Variation percentage δ_{cr}) %	Fire time (min)
—	LSS	Steel	Sold	72	55.8	—	—	—
Group	LSS	Steel	Sold	143.45	36.32	Reference	Reference	120
	LSC	Steel	Circular	188.44	20.24	31.36	-44.27	120
	LSQ	Steel	Square	168.14	27.73	17.21	-23.65	120
Group	LHS	Hybrid	Sold	155.86	39.75	Reference	Reference	120
	LHC	Hybrid	Circular	221.72	31.42	42.23	-20.91	120
	LHQ	Hybrid	Square	174.37	35.3	11.86	-11.211	120
Group	LGS	GFRP	Sold	93.98	91.72	Reference	Reference	50
	LGC	GFRP	Circular	102	83.17	8.52	-9.31	70
	LGQ	GFRP	Square	97.6	85.24	3.83	-7.05	80

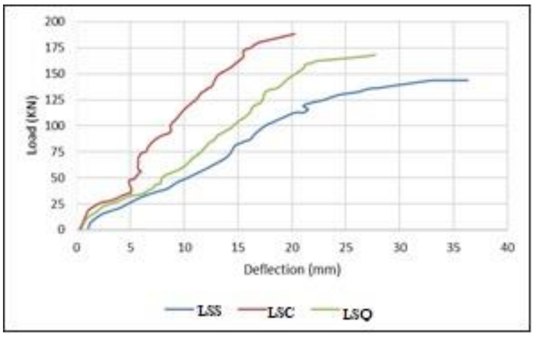

a- Load-Deflection for steel reinforcement

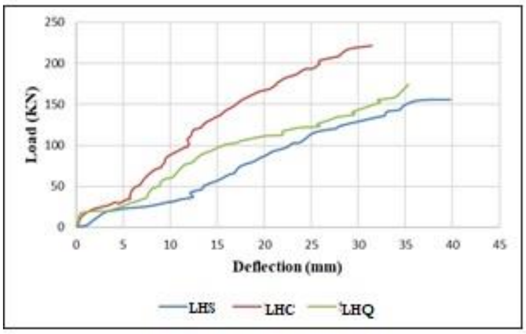

b- Load-Deflection for hybrid reinforcement

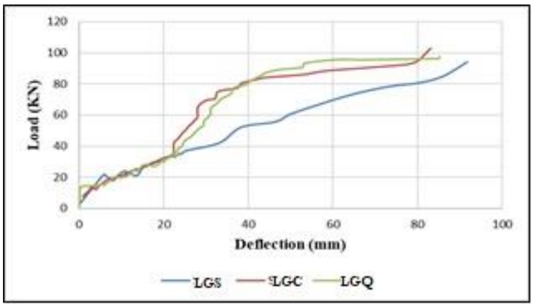

c- Load-Deflection for GFRP reinforcement

Fig. 8. Ultimate Load-Deflection relationship in hollow reinforced LWC slabs.

3.2.3. Ductility

The ductility index, a measure derived from a material's load-deflection curve, quantifies the ratio of deflection at ultimate load to deflection at the yield point, marking the transition from elastic to plastic deformation (Lees and Burgoyne, 1999; Salih, 2023). Table 5 and Fig. 9 present the calculated ductility indices for one-way hollow concrete slabs, comparing those reinforced with steel, hybrid systems, and GFRP with different void shapes.

The results demonstrate that the presence of hollows affects the ductility of the slabs. For instance, compared to the reference solid slab (LSS), which had a ductility index of 3.51, the slab with circular voids (LSC) exhibited a 7.4% higher ductility, while the slab with quadrilateral voids (LSQ) showed a marginal increase of 1.13%. Incorporating a second layer of steel reinforcement in the compression zone was found to enhance ductility relative to the solid reference slab. This improvement effectively compensated for the reduction in concrete area due to the voids, resulting in overall greater ductility for the hollow reinforced concrete slabs.

Overall, slabs reinforced with GFRP bars exhibited low ductility and displayed brittle failure characteristics, which aligns with the typical behavior of GFRP-reinforced concrete.

3.2.4. Stiffness

Stiffness (K) refers to the ability of a one-way slab to resist deformation. In reinforced concrete slabs, stiffness is evaluated using the "effective secant stiffness" method, which involves applying 45% of the maximum load (0.45 × Pu) to the load-deflection curve and recording the corresponding deflection (Duthinh and Starnes, 2004; Salih, 2023). The stiffness results for the tested slabs are provided in Table 6 and compared under static and fire conditions in Fig. 10. The data show that elevated temperatures during firing led to a reduction in slab stiffness. The use of lightweight concrete was also found to decrease stiffness. Moreover, as the first cracks appeared, the rigidity of slabs strengthened with GFRP bars drastically decreased. Compared to slabs reinforced with steel, these fissures were much deeper and broader. Although reinforced GFRP slabs developed fewer cracks, the cracks were more severe, facilitating heat transfer to the bars and accelerating failure.

In contrast, steel-reinforced slabs had a greater number of smaller, less widespread fractures. Crack width increased significantly beyond the yield point, indicating ongoing structural degradation.

Table 5. Ductility values of lightweight, hollow concrete slabs.

Group	Symbols	Type of Reinf.	Shape of hollow	Steel Yielding Load (KN)	Ultimate Load (Pu)(KN)	Deflection Yield (δy) (mm)	Deflection Yield (δu) (mm)	Ductility (δu/δy)
—	LSS	Steel	Sold	45.12	72	____	____	____
Group1	LSS	Steel	Sold	41.93	143.45	10.34	36.32	3.51
	LSC	Steel	Circular	35.53	188.44	5.36	20.24	3.77
	LSQ	Steel	Square	37.23	168.14	7.79	27.73	3.55
Group2	LHS	Hybrid	Sold	48.21	155.86	11.03	39.76	3.6
	LHC	Hybrid	Circular	41.21	221.71	5.96	31.43	5.27
	LHQ	Hybrid	Square	45.21	174.38	8.14	35.3	4.33
Group3	LGS	GFRP	Sold	56.99	93.98	40.16	91.71	2.28
	LGC	GFRP	Circular	73.44	102	36.45	83.16	2.28
	LGQ	GFRP	Square	77.86	97.6	37.14	85.23	2.29

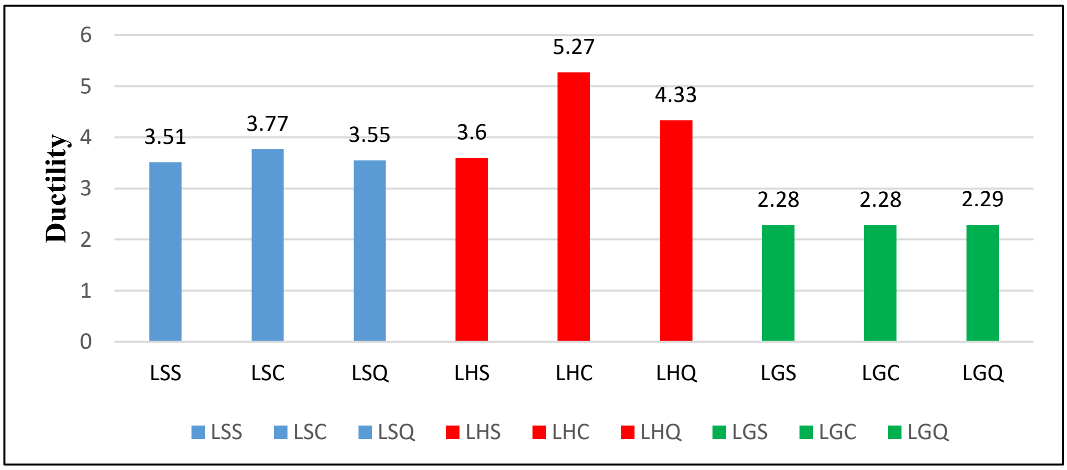

Fig. 9. Comparing the ductility values of hollow light-weight concrete slabs.

Table 6. Stiffness of the evaluated lightweight hollow concrete slabs.

Group	Symbols	Type of Reinf.	Shape of hollow	Ultimate Load Pu (KN)	Service load = 0.45*Pu (KN)	Deflection at Service load, δ (mm)	Stiffness, k = P/δ (KN/mm)
-	LSS	Steel	Sold	72	______	_____	Without fire
Group 1	LSS	Steel	Sold	143.45	64.55	13.56	4.76
	LSC	Steel	Circular	188.44	84.79	8.86	9.46
	LSQ	Steel	Square	168.14	75.66	12.29	6.15
Group 2	LHS	Hybrid	Sold	155.85	70.12	16.55	4.22
	LHC	Hybrid	Circular	221.72	99.75	12.92	7.73
	LHQ	Hybrid	Square	174.37	78.47	11.52	6.82
Group 3	LGS	GFRP	Sold	93.97	42.28	32.2	1.32
	LGC	GFRP	Circular	102	45.91	25.22	1.82
	LGQ	GFRP	Square	97.61	43.93	24.31	1.8

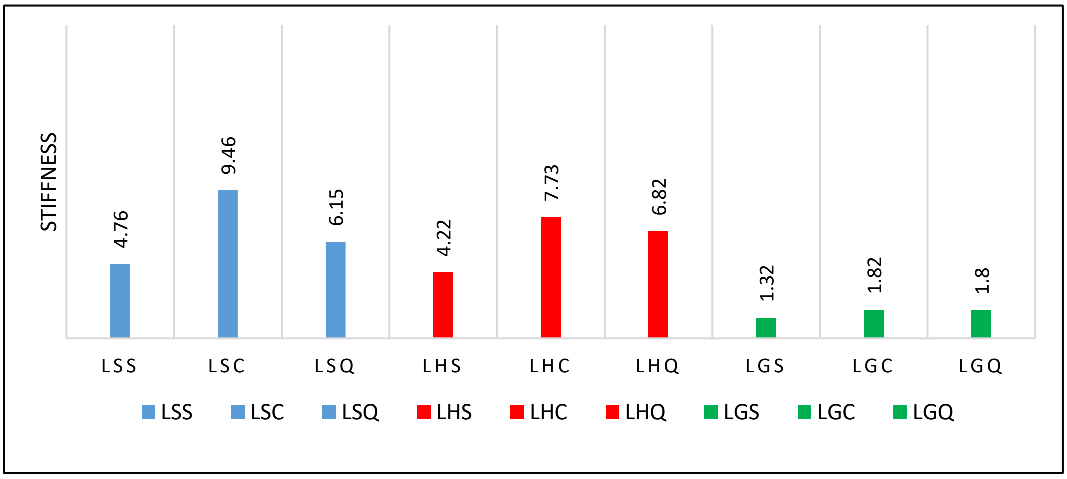

Fig. 10. Comparing the stiffness values of hollow light-weight concrete slabs

3.2.5. Failure patterns

The initial cracking consistently occurred in the mid-span region between the supports. This area, being a zone of pure bending with minimal shear stress, led to the development of cracks perpendicular to the tensile bending stresses. Fig. 11 displays the characteristic crack patterns for both solid and hollow reinforced concrete slabs. Under increasing load, the flexural cracks on the tensile face of the slabs propagated and widened, with observable variations in crack width between the solid and hollow specimens.

While the failure of the concrete slabs reinforced with steel reinforcement was caused by an increase in the slab's curvature without experiencing sudden failure, the failure of all slabs reinforced with GFRP bars was caused by the extension of one crack in the moment region and the breaking of the GFRP bars at the ultimate load.

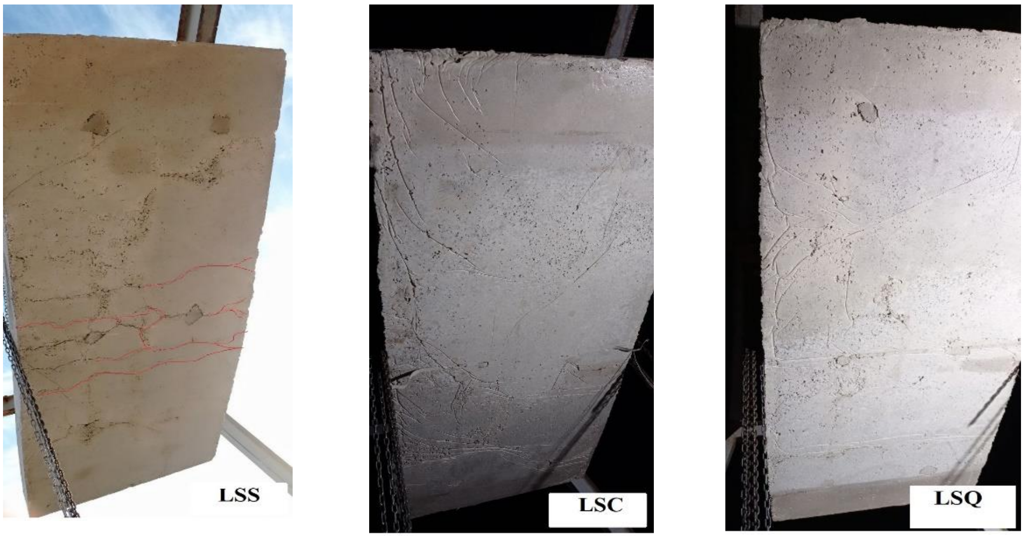

Group 1. One-way hollow lightweight concrete slabs with steel reinforcement

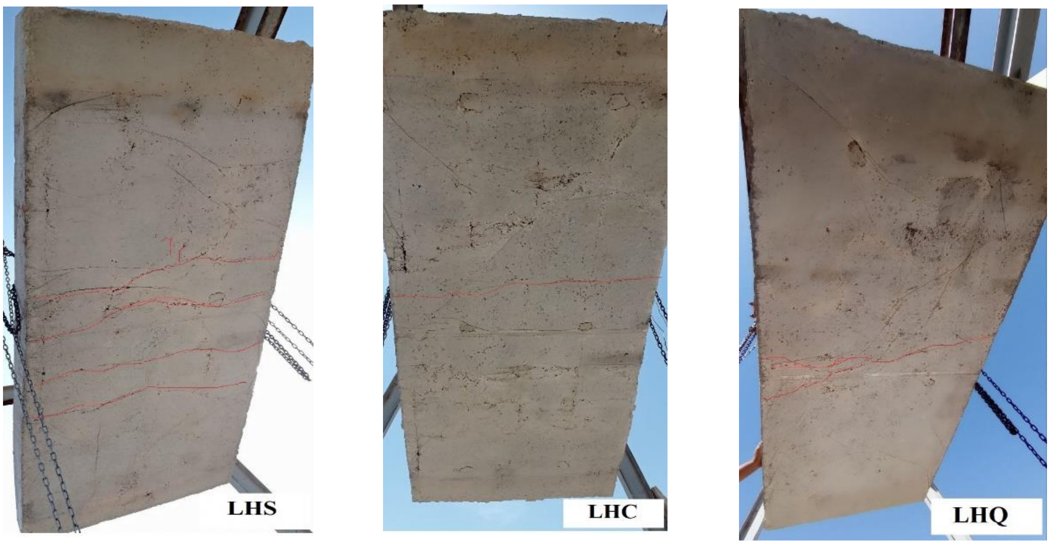

Group 2. One-way hollow lightweight concrete slabs with hybrid reinforcement

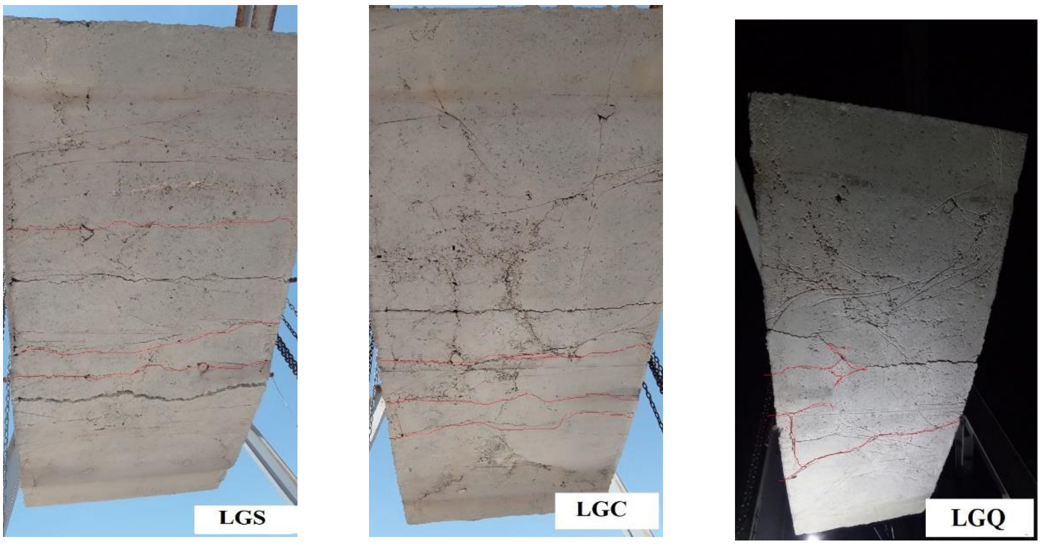

Group 3. One-way hollow lightweight concrete slabs with GFRP reinforcement

Fig. 11. Show failure patterns for all hollow lightweight concrete slabs reinforced with steel, hybrid, and GFRP.

4. CONCLUSIONS

The following findings may be made from the experimental study of how hollow, lightweight concrete slabs reinforced with steel, hybrid, and GFRP systems behave in high-temperature environments:

• A significant reduction of 35% in the maximum flexural capacity was observed in GFRP-reinforced lightweight concrete slabs (LGS) exposed to temperatures exceeding 800°C for 120 minutes, compared to their steel-reinforced counterparts.

• Slabs with GFRP reinforcement demonstrated considerable deflection under very high temperatures.

• GFRP bars exhibited a slow heating rate, reaching a maximum temperature of only 200°C after 50 minutes of exposure to fires above 800°C.

• Elevated firing temperatures resulted in decreased stiffness and ductility across all slabs. Although a higher GFRP reinforcement ratio further reduced stiffness, its effect on ductility was negligible.

• Flexural cracks formed in GFRP-reinforced slabs at high temperatures (more than 800°C), even when subjected to low loads within the elastic range.

• All slabs ultimately failed in flexure due to extensive yielding of the tensile reinforcement, characterized by significant cracking without major concrete spalling in the compression zone. The initial bottom-surface cracks, which ran parallel to the supports, were attributed to thermal fracturing of the flooring material.

- For future research on the flexural behavior of LWC slabs under combined static and fire loads, the following directions are proposed:

• Further studies should examine the performance of lightweight concrete slabs incorporating steel and polypropylene fibres, particularly to assess their fire resistance when exposed to multi-sided fires.

• Research should be extended to evaluate the fire performance of other structural elements reinforced with GFRP bars, including columns, beams, and T-beams.

• The scope of inquiry could be broadened to include slabs reinforced with alternative materials such as carbon FRP, basalt FRP, and geopolymer composites, analyzing their performance under simultaneous fire and loading conditions.

ACKNOWLEDGEMENTS

The authors would like to express their gratitude to Tikrit University, specifically the College of Engineering, Department of Civil Engineering, for funding this study. This research was supported by the grant provided under the University Order dated March 15, 2021, for enrolment in postgraduate studies (3543-7-3).

5. REFERENCE

Abdullah, A.N. and Kassim, M.M. (2024) “Residual Strength of Concrete Beams Reinforced with GFRP Bars Exposed to Elevated Temperatures,” Tikrit Journal of Engineering Sciences, 31(3), pp. 18–31. Available at: https://doi.org/10.25130/tjes.31.3.3.

Al-Attar, A.A., Abdulrahman, M.B., Hamada, H.M. and Tayeh, B.A. (2020) “No TitleInvestigating the behaviour of hybrid fibre-reinforced reactive powder concrete beams after exposure to elevated temperatures,” J. Mater. Res. Technol, 9(2), pp. 1966–1977.

Badawi, A. et al. (2023) “Structural Behavior of Hollow Beam Reinforced with Different Types of GFRP Stirrups.,” iasj.netAK Badawi, YIO Yahia, AI AbdullaTikrit Journal of Engineering Sciences, 2023•iasj.net, 30(1), pp. 72–83. Available at: https://doi.org/10.25130/tjes.30.1.7.

Chaturvedi, S., Vedrtnam, A., Youssef, Maged A, et al. (2022) “Fire-resistance testing procedures for construction elements—A Review,” mdpi.comS Chaturvedi, A Vedrtnam, MA Youssef, MT Palou, G Barluenga, K KalauniFire, 2022•mdpi.com, 6(1). Available at: https://doi.org/10.3390/fire6010005.

Chaturvedi, S., Vedrtnam, A., Youssef, Maged A., et al. (2022) “Fire-Resistance Testing Procedures for Construction Elements—A Review,” Fire, 6(1), p. 5. Available at: https://doi.org/10.3390/FIRE6010005.

Duthinh, D. and Starnes, M. (2004) “Strength and Ductility of Concrete Beams Reinforced with Carbon Fiber-Reinforced Polymer Plates and Steel,” Journal of Composites for Construction, 8(1), pp. 59–69. Available at: https://doi.org/10.1061/(asce)1090-0268(2004)8:1(59).

Ftnan, A.H. and Makki, R.F. (2022) “BEHAVIOR OF RECYCLED AGGREGATE CONCRETE BEAMS STRENGTHENED WITH FRP,” Kufa Journal of Engineering, 13(4), pp. 13–24. Available at: https://doi.org/10.30572/2018/KJE/130402.

Hibtallah, E. and K. Madlum, M. (2022) “DYNAMIC BEHAVIOR OF SLAB REINFORCED WITH FRP BARS AND STRENGTH WITH CARBON SHEET,” Kufa Journal of Engineering, 13(1), pp. 64–81. Available at: https://doi.org/10.30572/2018/KJE/130104.

Ibrahim, R.K. and Lateef, A.M. (2024) “Flexural behavior of corroded one-way slabs strengthened with CFRP in two different techniques,” Innovative Infrastructure Solutions, 9(9). Available at: https://doi.org/10.1007/S41062-024-01648-6.

Jasim, A.T. and Jabal, Q.A. (2010) “NO-FINE LIGHTWEIGHT AGGREGATE CONCRETE MODIFIED WITH STYRENE BUTADIENE RUBBER,” Kufa Journal of Engineering, 1(2), pp. 32–44. Available at: https://doi.org/10.30572/2018/KJE/121299.

Jomaa’h, M. et al. (2019) “Mechanical and structural properties of a lightweight concrete with different types of recycling coarse aggregate,” iasj.netMM Jomaa’h, BT Kamil, OS BaghabraTikrit Journal of Engineering Sciences, 2019•iasj.net [Preprint]. Available at: https://doi.org/10.25130/tjes.26.1.05.

Jomaa’h, M.M., Ahmed, S. and Algburi, H.M. (2018) “Flexural Behavior of Reinforced Concrete One-Way Slabs with Different Ratios of Lightweight Coarse Aggregate,” Tikrit Journal of Engineering Sciences, 25(4), pp. 37–45. Available at: https://doi.org/10.25130/TJES.25.4.07.

Klak, F.S. and Jomaa’h, M.M. (2024) “Conventional and lightweight aggregate one-way reinforced concrete slabs subjected to fire and repeated loads: comparative experimental study,” Australian Journal of Structural Engineering, 25(1), pp. 106–123. Available at: https://doi.org/10.1080/13287982.2023.2213504.

Lees, J.M. and Burgoyne, C.J. (1999) “Experimental study of influence of bond on flexural behavior of concrete beams pretensioned with aramid fiber reinforced plastics,” ACI Structural Journal, 96(3), pp. 377–385. Available at: https://doi.org/10.14359/671.

Momtazi, A.S. et al. (2015) “Pozzolans’ Effect on Durability of Light Concretes Made of LECA (Light Expanded Clay Aggregate) and Scoria in Corrosive Environments Containing Sulfuric acid,” European Online Journal of Natural and Social Sciences: Proceedings, 4(3(s)), pp. 101–109.

Murthy, A.R., Pukazhendhi, D.M., Vishnuvardhan, S., Saravanan, M. and Gandhi, P. (2020) “Performance of concrete beams reinforced with GFRP bars under monotonic loading,” Structures, 27, pp. 1274–1288. Available at: https://doi.org/10.1016/J.ISTRUC.2020.07.020.

Nimnim, H. and Zain Alabdeen, Z. (2021) “STRUCTURAL BEHAVIOR OF VOIDED NORMAL AND HIGH STRENGTH REINFORCED CONCRETE SLABS,” Kufa Journal of Engineering, 10(2), pp. 1–11. Available at: https://doi.org/10.30572/2018/KJE/100201.

Rosa, I.C., Firmo, J.P., Correia, J.R. and Bisby, L.A. (2023) “Fire Behavior of GFRP-Reinforced Concrete Structural Members: A State-of-the-Art Review,” Journal of Composites for Construction, 27(5). Available at: https://doi.org/10.1061/JCCOF2.CCENG-4268.

Sajedi, F. and Shafigh, P. (2012) “High-Strength Lightweight Concrete Using Leca, Silica Fume, and Limestone,” Arabian Journal for Science and Engineering, 37(7), pp. 1885–1893. Available at: https://doi.org/10.1007/S13369-012-0285-3/METRICS.

Salih, Y.A., Al-Salman, H.A., Jomaa’h, M.M. and Abdulla, A.I. (2023) “Flexural Behavior of Reinforced Concrete Voided Slabs Strengthened with Different Types of FRP: State-of-the-Art Review,” tj-es.comYA Salih, HA Al-Salman, MM Jomaa’h, AI AbdullaTikrit Journal of Engineering Sciences, 2023•tj-es.com, 30(3), pp. 124–139. Available at: https://doi.org/10.25130/tjes.30.3.13.

Salih, Y.A. (2023) Flexural Behavior of Reinforced Concrete Voided One-Way Slabs with Steel and GFRP Bars. Ph.D. Thesis, University of Tikrit; Tikrit,Iraq.

Setareh, M. and Darvas, R. (2017) “Rectangular Beams and One-Way Slabs,” Concrete Structures, pp. 37–149. Available at: https://doi.org/10.1007/978-3-319-24115-9_2.

Standard, A.C.I. (1996) “Standard practice for selecting proportions for normal, heavyweight, and mass concrete,” ACI Man. Concr. Pract, 1996, pp. 1–38.

Tanano, H., Masuda, Y., Kage, T., Fukuyama, H., Nishida, I. and Hashimoto, T. (1995) “Fire resistance of continuous fibre reinforced concrete in non-metallic (FRP) reinforcement for concrete structures,” Taerwe (eds), E&FN Spon, London, United Kingdom, p. 9.